Bioorganic Chemistry 86 (2019) 97–102

Contents lists available at ScienceDirect

Bioorganic Chemistry

journal homepage: www.elsevier.com/locate/bioorg

Identification of *ortho*-naphthoquinones as anti-AML agents by highly efficient oxidation of phenols

Huidan Huang[a], Ming Yan[a], Jianqiu Chen[a], Biao Yuan[c], Guitang Chen[c], Shujie Cheng[c], Dechun Huang[a], Zhen Gao[b,*], Chongjiang Cao[a,*]

[a] Department of Pharmaceutical Engineering, China Pharmaceutical University, Nanjing 210009, China
[b] College of Biotechnology and Pharmaceutical Engineering, Nanjing Tech University, Nanjing 211816, China
[c] Department of Food Quality and Safety, School of Engineering, China Pharmaceutical University, Nanjing 211816, China

A B S T R A C T

A straightforward method for synthesizing *ortho*-naphthoquinones was identified using an easily available cobalt–Schiff base complex. Efficient oxidation of phenols to *ortho*-naphthoquinones was useful in obtaining compounds with potent biological activity for the treatment of acute myeloid leukemia (AML). Among these compounds, the compound **4h** effectively inhibited the proliferation of different AML cell lines *in vitro*. Further *in vivo* antitumor studies indicated that **4h** at 40 mg/kg/d led to tumor regression in led to tumor regression in an MV4-11 xenograft model without evident toxicity. The cobalt-Schiff base complex was found to be an efficient catalyst in the transformation of phenols to *ortho*-quinones, and the compound **4h** represents a potential scaffold to optimize the production of a treatment for AML.

1. Introduction

Acute myeloid leukemia (AML) is one of the most common type of leukemia [1,2]. Cytotoxic or targeted drugs and hematopoietic stem cell transplant therapy is typically used to treat patients with AML. However, these therapies remain unsatisfactory with 3–8% survival at 5 years in patients aged more than 60 years and up to 50% in patients younger than 60 years [3,4]. Thus, an efficient and well-tolerated drug for the treatment of AML needs to be developed. The challenge to AML treatment is attributed to the heterogeneity of various leukemogenic mutations and cytogenetic abnormalities with a poorly understood interplay among them in each patient [5,6]. A therapy focused on targeting the broader characteristic of all AML cells would be an efficient method. Growing evidence shows that compared with normal cells, AMLs are characterized by high levels of oxidative stress relative to normal cells [7,8]. Oxidative stress is develop by reactive oxygen species (ROS) that accumulate as a result of an imbalance between ROS generation and elimination [9]. Numerous genetic changes that confer an elevated ROS phenotype occur within AML. An elevated basal ROS level increases the susceptibility of AML cells to exogenously induced ROS-mediated cell death [7,10]. Potentiating ROS in cancers by using small molecules has been regarded as a rational approach to drug design in order to strengthen the relationship between ROS and AML [11,12].

Ortho-naphthoquinones, such as Tanshinone IIA and β-lapachone are most widely investigated anticancer agents for solid tumors (Fig. 1) [13]. Our cooperated group has synthesized several *ortho*-naphthoquinones with potent antitumor activity against non-small cell lung cancer [12–15]. Several quinones have recently been found to efficiently treat AML [8,16,17]. We committed to develop *ortho*-naphthoquinones as novel effective antitumor agents with a superior safety profile. An in-depth study of these *ortho*-naphthoquinones as treatment for AML has not been conducted; thus, we intended to evaluate their activity in order to obtain a potential treatment for AML.

In the present study, we focused on developing a novel method to construct *ortho*-naphthoquinones before evaluating the biological activity of these compounds. Substantial research has focused on the synthesis of *ortho*-naphthoquinones. In the process of constructing the naphthoquinone scaffold, oxidation of phenolics or amines to form the quinone scaffold plays a key role. Accordingly, a large number of oxidation agents have been identified. Classical methods use Fremy's salt $K_2(SO_3)_2NO$ or HNO_3, as well as hypervalent iodine derivatives such as IBX [18–20]. Although several of these oxidants are efficient, however, these methods have disadvantages, such as low yield, and induces undesirable side effects.

Cobalt–Schiff base complexes, which are known to reversibly bind oxygen, have been commonly used to catalyze oxygen activation in the oxidation of phenols to *para*-quinones [21]. However, studies on the use of these complexes to oxidize *ortho*-naphthoquinones as catalytic conversion models of naphthol have rarely been reported. Using easily

* Corresponding authors.
E-mail addresses: gaozhen@njtech.edu.cn (Z. Gao), ccj33@163.com (C. Cao).

https://doi.org/10.1016/j.bioorg.2019.01.025
Received 11 September 2018; Received in revised form 12 January 2019; Accepted 12 January 2019
Available online 18 January 2019
0045-2068/ © 2019 Elsevier Inc. All rights reserved.

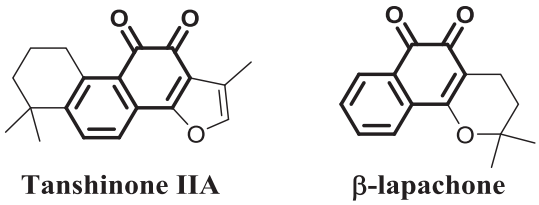

Fig. 1. Structures of representative *ortho*-naphthoquinone compounds.

available Co(salen) (**1**, **2**), we demonstrated the oxidation of phenols leading to a straightforward method for synthesizing *ortho*-naphthoquinones (Fig. 2). The obtained *ortho*-naphthoquinones were also screened for cytotoxicity against AML cells. *In vivo* antitumor studies were performed to evaluate the efficacy of the most potent compound.

2. Synthetic methodology

We initially investigated the reaction conditions for 3-methyl-5-hydroxynaphthol[1,2-*b*]furan (**3a**) as a model substrate. By using O_2 with 10% of catalysts **1** or **2** to treat **3a**, *ortho*-naphthoquinone (**4a**) was obtained at 50% and 52% yields, respectively. Further reducing the amount of catalyst **1** to 5% prompts a significant decrease in **4a** yield; meanwhile, reducing catalyst **2** to 5% and shortening the reaction time to 5 h result in nearly the same **4a yield** (entries 3–4). Thus, catalyst **2** exhibits higher reactivity, compared with **1**. The moderate reactivity of catalyst **1** may be attributed to its poor oxygen-binding capacity. Thus, catalyst **2** was selected for further study. No considerably increase in yield was observed when the temperature was set higher than the room temperature (entries 5–7). The presence of additional aromatic or aliphatic nitrogen bases reportedly enhanced the reactivity of the catalytically active complex [21]. The effect of adding an axial ligand was then evaluated. The yield of *ortho*-naphthoquinone (**4a**) from naphthol was significantly improved by adding a base *N*,*N*-diisopropylethylamine, pyridine, or triethylamine (TEA) to oxidations catalyzed by **2** (entries 8–10). Oxidation of **3a** by using catalytic amounts of Co(salen) and equimolar amounts of TEA obtains the highest yield (70%) of **4a**. We then evaluated the effect of solvents and determined that CH_3CN/H_2O was the best solvent for this reaction among those tested (entries 11–15). Therefore, the optimized reaction conditions consist of **2** (10 mol %), TEA (100 mol %), and CH_3CN/H_2O (solvent) at room temperature for 2 h under O_2 (50 psi) (Table 1).

With the optimized reaction conditions in hand, other *ortho*-naphthoquinones were systematically screened. In Scheme 1, naphthol derivatives are successfully transformed into the desired products in moderate to high yields. Most naphthols were synthesized as described in previous studies, with moderate to high yields [12–15]. The naphthol **3h** was synthesized as shown in Scheme 2 [13,22].

Notably, the effectiveness of **2** as a catalyst was also demonstrated by the oxidation of nitrogen-containing heteroaromatic naphthol substrate **3h** to the quinone **4h** in high yield. The model **3h** yielded

Table 1
Condition screening for oxidation of phenol **3a** into quinone **4a**.[a]

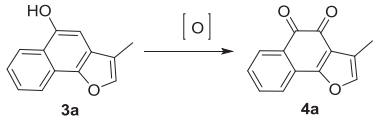

Entry	Catalyst	Additive	Solvent	Time (h)	T	Conv.(%)
1	**1**	–	MeOH	2	r.t.	50
2	**2**	–	MeOH	2	r.t.	52
3[b]	**1**	–	MeOH	5	r.t.	31
4[b]	**2**	–	MeOH	5	r.t.	48
5	**2**	–	MeOH	2	35	60
6	**2**	–	MeOH	2	45	63
7	**2**	–	MeOH	2	60	58
8	2	DIPEA	MeOH	2	r.t.	62
9	2	Pyr	MeOH	2	r.t.	58
10	2	TEA	MeOH	2	r.t.	70
11	2	TEA	CH_3CN	2	r.t.	85
12	2	TEA	EtOH	2	r.t.	63
13	2	TEA	CH_3CN/H_2O	2	r.t.	92
14	2	TEA	CH_2Cl_2	2	r.t.	70
15	**2**	Pyr	CH_3OH/CH_2Cl_2	3	r.t.	78

[a] Reaction conditions: **3a** (0.50 mmol), catalyst **2** (10 mol %) under O_2 (50 psi).

corresponding product in similar amounts although a longer reaction time and higher catalyst loadings were required. To demonstrate the practicability of the method, the model procedure was successfully scaled up with comparable yield. The product **4a** (1.85 g, 79%) was prepared when the reaction was run in a 10 mmol scale (Scheme 3).

A possible catalytic cycle for these reactions, employing the model substrate **3a** for illustrative purposes, is shown in Scheme 4. The first starting cobalt–Schiff base/ligand complex **A** is converted to the superoxo complex **B** upon reaction with O_2 [23,24]. Reacting **B** with the model substrate **3a** then generates the phenoxy radical **C** and **D**, which is transformed into the intermediate **E**, followed by elimination of water and the product **4a**. The mediate **F** was further oxidized to regenerate the catalyst **B**.

3. Biological activity

3.1. In vitro cytotoxic activity screening

When these compounds were obtained with good yields, we investigated the antiproliferative activity of these *ortho*-naphthoquinones against AML cells by MTT assay. We observed that most *ortho*-naphthoquinones exhibited moderate to high activities toward these AML cell lines (MV4-11, MOLM-14, and THP-1) (Table 2). Except for compound **4e** and **4f**, which showed poor activity toward all of the three

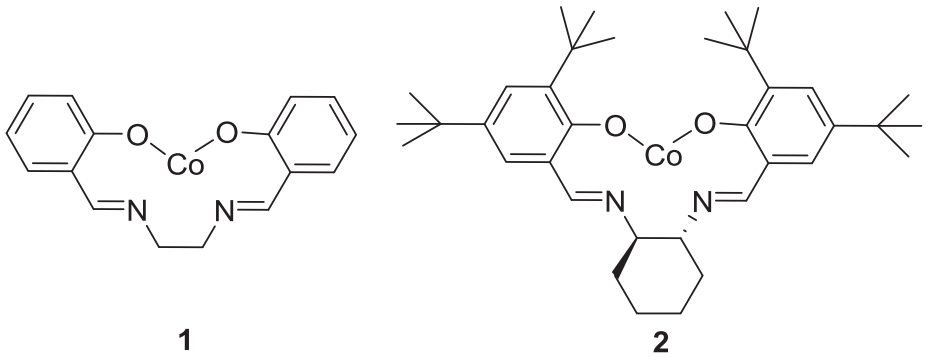

Fig. 2. Structures of cobalt–Schiff base complexes used in this study.

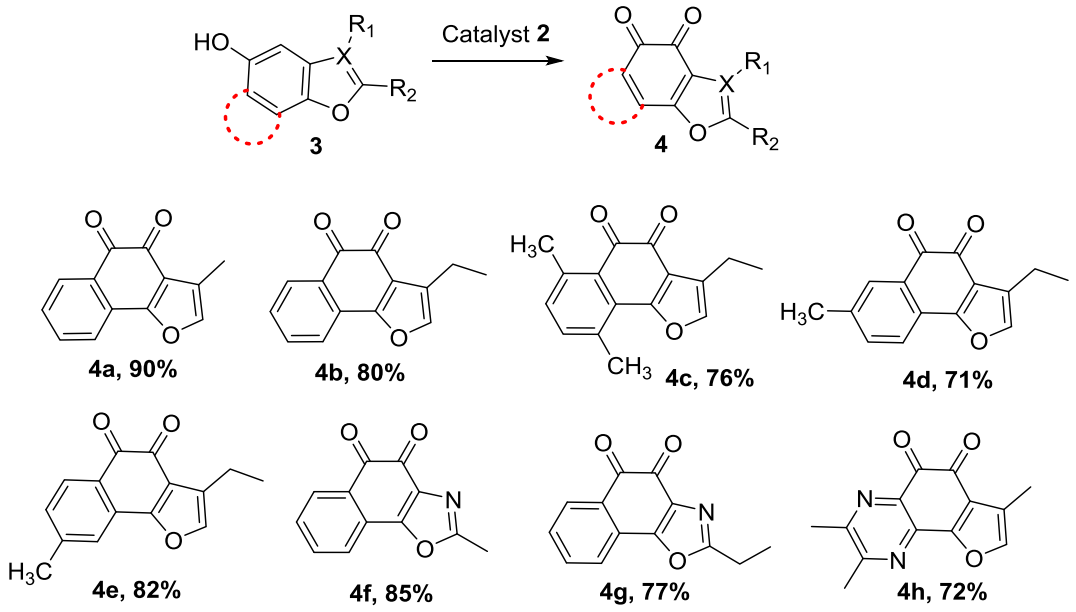

Scheme 1. Substrate scope of *ortho*-naphthoquinones. Reaction conditions: catalyst **2** (0.05 mmol), **3** (0.5 mmol), TEA (0.5 mmol) in CH_3CN/H_2O for 2 h at room temperature for 2 h under O_2 (50 psi). Isolated yield.

cell lines. Most of the methyl-substituted naphtho[1,2-*b*]furan-4,5-diones **4b-4d** showed more potent activity than compound **4a** toward MV4-11 cells. When introducing the nitrogen atom into the benzene ring (compound **4h**), the cytotoxicity toward MV4-11 is significantly improved (IC_{50} = 0.11 ± 0.07 μM). In addition, the 2-ethyl naphtho [2,1-*d*]oxazole-4,5-diones (**4g**) also showed good activity with IC_{50} = 0.41 μM toward MV4-11 cells. As for the MOLM-14 cell lines, only three compounds (**4c**, **4g** and **4h**) showed inhibitory activity. This result indicated that the *ortho*-quinone maybe the key pharmacophore for their antitumor activity due to the A ring or C ring are different with each other of these three compounds. Compounds **4a-4c** showed more inhibitory activity against THP-1 compared with single methyl-substitution at the benzene ring (**4d** and **4e**). Among these compounds, **4g** and **4h** showed potent inhibitory activity toward all these three cell lines, probably due to the improved physicochemical properties. Specifically, the compound **4h** showed a concentration-dependent decrease after exposure for 48 h with IC_{50} values of 0.11 ± 0.07 μM for MV4-11, 0.65 ± 0.12 μM for MOLM-14, and 0.60 ± 0.14 μM for THP-1 (Fig. 3).

3.2. In vivo antitumor activity study.

The compound **4h** exhibited superior potency; thus, it was selected for further *in vivo* evaluation. The oral efficacy of **4h** was evaluated in a xenograft model in athymic nude mice with a subcutaneous implant of an MV4-11 cell pellet (Fig. 4). When the tumors grew to ~150 mm^3, the animals were randomly injected with a vehicle, **4h** (20 and 40 mg/kg), and the control sunitinib (40 mg/kg) once a day for three weeks. At both doses of **4h**, the tumor growth of implanted AML tumor was inhibited ($p < 0.01$ vs. the vehicle-treated control, Fig. 4). The compound **4h** (40 mg/kg) demonstrated potent *in vivo* antitumor activity with tumor growth inhibition (63.4%) comparable to that of sunitinib (40 mg/kg, 66.8%). In addition, no body weight loss was observed in animals treated with **4h** compared with the vehicle (Fig. 4B). These

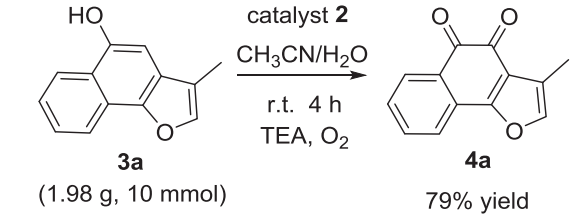

Scheme 3. Scale-up experiment.

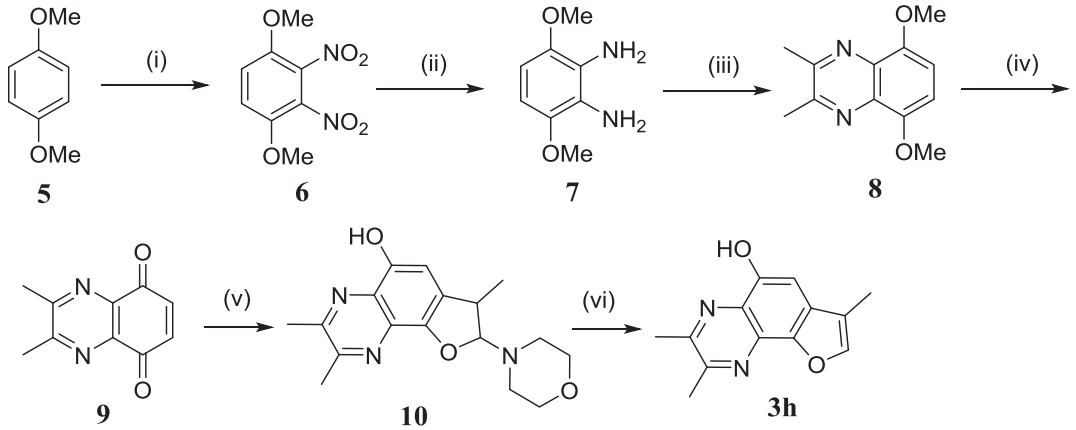

Scheme 2. Reactions and conditions. (i) HNO_3 (62%), 0 °C to r.t., 3 h, 90% yield. (ii) H_2, Pd/C, r.t., 6 h, 92% yield. (iii) freshly distilled 2,3-butanedione, reflux, 30 min, 85% yield. (iv) ceric ammonium nitrate, r.t., 1 h. 95% yield. (v) CH_2Cl_2, 0 °C to r.t., 12 h, 55% yield. (vi) dil. HCl, 75 °C, 3 h, 80% yield.

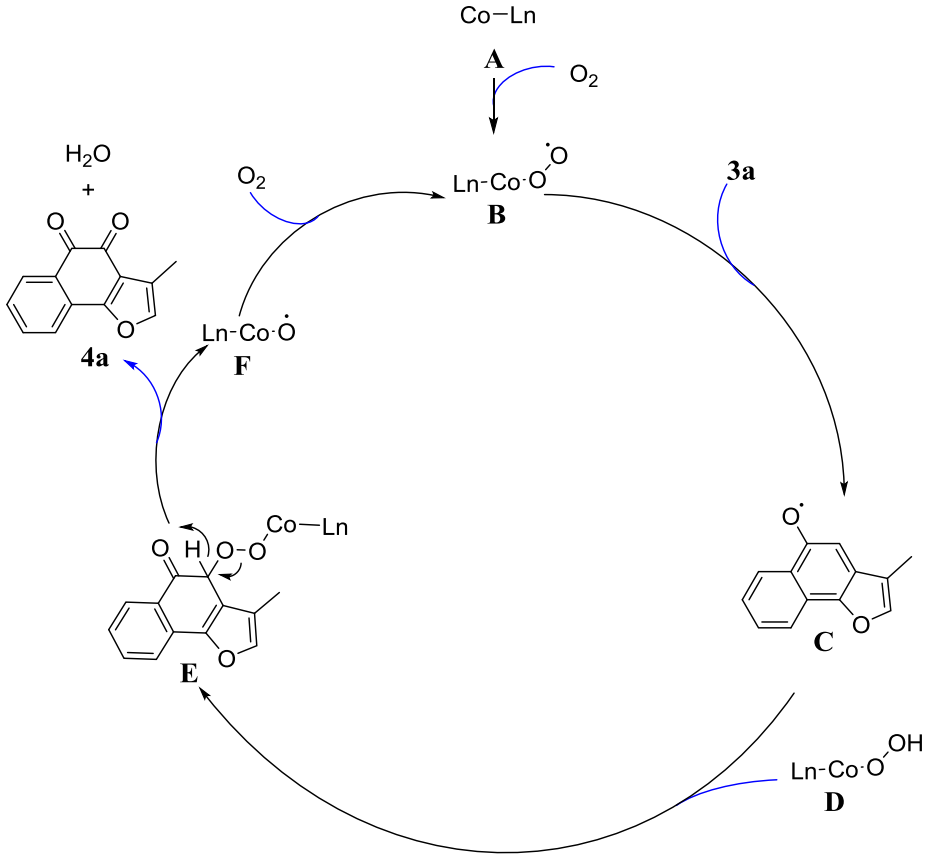

Scheme 4. Proposed mechanism for *ortho*-naphthoquinone formation from naphthol catalyzed by the catalyst Co.

Table 2
In vitro antitumor activity of compounds **4a-4h**[a].

Entry	Compound	MV4-11 (μM)	MOLM-14 (μM)	THP-1 (μM)
1	**4a**	> 10	> 10	5.81 ± 0.82
2	**4b**	7.98 ± 1.82	> 10	6.12 ± 1.03
3	**4c**	7.10 ± 0.98	6.20 ± 1.12	4.19 ± 0.89
4	**4d**	9.21 ± 1.68	> 10	> 10
5	**4e**	> 10	> 10	> 10
6	**4f**	> 10	> 10	> 10
7	**4 g**	0.41 ± 0.10	4.98 ± 0.31	1.50 ± 0.64
8	**4h**	0.11 ± 0.07	0.65 ± 0.12	0.60 ± 0.14

[a] For the detailed structures of compounds **4a-4h**, see Scheme 1.

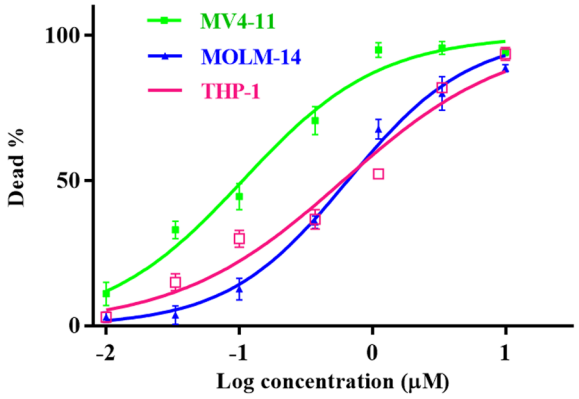

Fig. 3. Cell proliferation of different AML cells (MV4-11, MOLM-14 and THP-1) treated with compound **4h**.

results clearly demonstrated the efficacy and tolerability of the novel *ortho*-quinone scaffold **4h** in MV4-11 nude mice xenograft models.

4. Conclusion

In conclusion, we described a simple, efficient and scalable method for the oxidation of phenols to quinones. The efficient oxidation of phenols to *ortho*-quinones in this study helped obtain a series of compounds with efficient biological activity for the treatment of AML. In addition, the compound **4h** exhibited efficacy both *in vitro* and *in vivo*. These findings encourage further investigations around the *ortho*-naphthoquinones. We aim to identify the optimal *ortho*-naphthoquinones for the treatment of AML in clinicals.

5. Experimental section

5.1. Chemistry

5.1.1. General experimental methods

Reactions were monitored by thin-layer chromatography on silica gel plates (60F-254) visualized under UV light. Melting points were determined on a Mel-TEMP II melting point apparatus without correction. ^{1}H NMR and ^{13}C NMR spectra were recorded in $CDCl_3$ on a Bruker Avance 300 MHz spectrometer at 300 MHz and 75 MHz, respectively. Chemical shifts (δ) are reported in parts per million (ppm) from tetramethylsilane (TMS) using the residual solvent resonance ($CDCl_3$: 7.26 ppm for ^{1}H NMR, 77.16 ppm for ^{13}C NMR. Multiplicities are abbreviated as follows: s = singlet, d = doublet, t = traplet, q = quartet, m = multiplet). IR spectra were recorded on a Nicolet iS10 Avatar FT-IR spectrometer using KBr film. MS spectra were recorded on a LC/MSD TOF HR- MS Spectrometer. Flash column chromatography was performed with 100–200 mesh silica gel and yields refer to

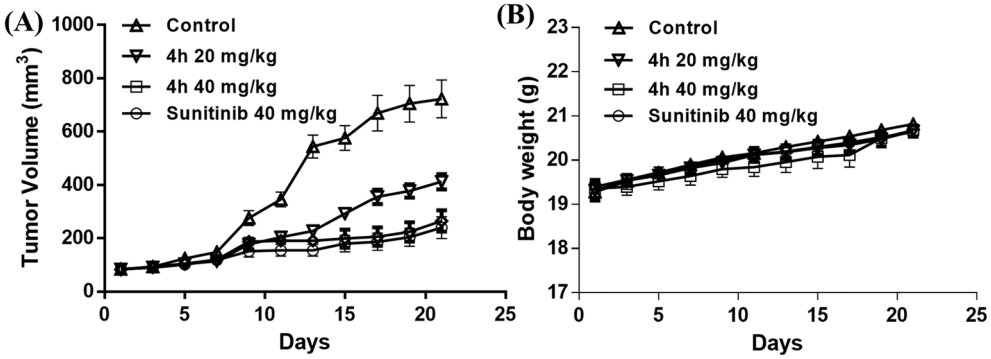

Fig. 4. Compound **4h** retards the tumor growth *in vivo* in MV4-11 xenografts nude ($p < 0.05$). (A) The tumor volume measurement. (B) Body weight measurement.

chromatographically and spectroscopically pure compounds.

All chemicals purchased from commercial suppliers were used as received unless otherwise stated. Reactions and chromatography fractions were monitored by Merck silica gel 60 F-254 glass TLC plates. All solvents were reagent grade and, when necessary, were purified and dried by standard methods.

5.2. Experimental procedures

5.2.1. Procedure for the preparation of 4a-4h

To a solution of o-phenol substrates (**3**, 0.5 mmol) and Co catalyst (0.05 mmol) were combined in 5 mL CH_3CN/H_2O in a Fisher-Porter bottle. The TEA (0.05 mmol) was added to the mixture and stirred for 15 min. The bottle was flushed with oxygen three times and then pressurized with oxygen to 50 psi and stirred at room temperature. After the reaction finished, the mixture was poured into cooled water (50 mL), extracted with ethyl acetate (3 × 100 mL), and washed with brine (100 mL). The organic layer was combined, dried over sodium sulfate, and concentrated under reduced pressure. The residue was purified by column chromatography on silica gel to provide the desired products.

5.2.2. Synthesis

3-Methylnaphtho[1,2-b]furan-4,5-dione ***(4a)***. m.p. 170–172 °C. ^{1}H NMR (300 MHz, $CDCl_3$) δ: 8.09 (d, J = 7.8 Hz, 1H), 7.69–7.62 (m, 2H), 7.47 (t, J = 9.0 Hz, 1H), 2.31 (s, 3H). IR (ν, cm^{-1}): 3134, 1672, 1590, 1539, 1020. ESI-HRMS m/z $[M + Na]^+$ calculated for $C_{13}H_8O_3Na$: 235.0371, found: 235.0374. HPLC purity (80% methanol in water): t_R = 8.01 min, 99.62%.

3-Ethylnaphtho[1,2-b]furan-4,5-dione ***(4b)***. m.p. 220–222 °C. ^{1}H NMR (300 MHz, $CDCl_3$) δ: 8.06 (d, J = 7.5 Hz, 1H), 7.72–7.62 (m, 2H), 7.48–7.43 (m, 1H), 7.28 (s, 1H), 2.73 (q, J = 7.4 Hz, 2H), 1.26 (t, J = 7.4 Hz, 3H). IR (ν, cm^{-1}): 3415, 2971, 1677, 1215, 1088. ESI-HRMS m/z $[M + H]^+$ calculated for $C_{14}H_{11}O_3$: 227.0703, found: 227.0707.

3,6,9-Trimethylnaphtho[1,2-b]furan-4,5-dione ***(4c)***. m.p. 203–204 °C. ^{1}H NMR (300 MHz, $CDCl_3$) δ: 8.09 (d, 1H, J = 7.8 Hz), 7.69–7.62 (m, 2H), 7.47 (t, 1H, J = 9.0 Hz), 2.31 (s, 3H). IR (ν, cm^{-1}): 3416, 2360, 2342, 1670, 1507, 1242. ESI-HRMS m/z $[M + H]^+$ calculated for $C_{15}H_{13}O_3$: 241.0859, found: 241.0854.

3,7-Dimethylnaphtho[1,2-b]furan-4,5-dione ***(4d)***. m.p. 216–217 °C. ^{1}H NMR (300 MHz, $CDCl_3$) δ: 7.90 (s, 1H), 7.60 (d, J = 7.8 Hz, 1H), 7.46 (d, J = 7.1 Hz, 1H), 7.26 (d, J = 1.3 Hz, 1H), 2.44 (s, 3H), 2.31 (d, J = 1.2 Hz, 3H). IR (ν, cm^{-1}): 3416, 2963, 2926, 1675, 1091, 804. ESI-HRMS m/z $[M + H]^+$ calculated for $C_{14}H_{11}O_3$: 227.0703, found: 227.0701.

3,8-Dimethylnaphtho[1,2-b]furan-4,5-dione ***(4e)***. m.p. 192–193 °C. ^{1}H NMR (300 MHz, $CDCl_3$) δ: 7.96 (d, J = 8.1 Hz, 1H), 7.50 (s, 1H), 7.23 (s, 2H), 2.46 (s, 3H), 2.29 (s, 3H). IR (ν, cm^{-1}): 3447, 2360, 2342, 1673, 1223. ESI-HRMS m/z $[M + H]^+$ calculated for $C_{14}H_{11}O_3$: 227.0703, found: 227.0708.

2-Methylnaphtho[2,1-d]oxazole-4,5-dione ***(4f)***. m.p. 180–181 °C. ^{1}H NMR (300 MHz, $CDCl_3$) δ: 8.17 (d, J = 7.5 Hz, 1H), 7.72–7.70 (m, 2H), 7.60–7.54 (m, 1H), 2.67 (s, 3H). ^{13}C NMR (75 MHz, $CDCl_3$) δ: 179.8, 175.1, 161.6, 139.3, 137.5, 127.3, 124.2, 123.6, 122.7, 119.8, 119.3, 11.7. IR (ν, cm^{-1}): 3415, 2361, 1683, 1638, 1592, 1561, 1228, 1065, 1002, 839, 581. ESI-HRMS m/z $[M + Na]^+$ calculated for $C_{12}H_7NO_3Na$: 236.0318, found: 236.0312.

2-Ethylnaphtho[2,1-d]oxazole-4,5-dione ***(4g)***. m.p. 190–192 °C. δ: 8.09 (d, J = 7.8 Hz, 1H), 7.63 (d, J = 3.8 Hz, 2H), 7.50–7.45 (m, 1H), 2.90 (q, J = 7.6 Hz, 2H), 1.39 (t, J = 7.6 Hz, 3H). IR (ν, cm^{-1}): 3415, 1685, 1562, 1229, 1067, 838, 573. ESI-HRMS m/z $[M + Na]^+$ calculated for $C_{13}H_9NO_3Na$: 250.0475, found: 250.0470.

2,3,7-Trimethylfuro[2,3-f]quinoxaline-5,6-dione ***(4h)***. m.p. 178–179 °C. δ: 7.42 (s, 1H), 2.68 (s, 1H), 2.63 (s, 1H), 2.01 (s, 1H) IR (ν, cm^{-1}): 3425, 1678, 1089, 857, 773. ESI-HRMS m/z $[M + H]^+$ calculated for $C_{13}H_{11}N_2O_3$: 243.0764, found: 243.0768.

5.3. Biological experiments

5.3.1. Cytotoxicity studies

Growth inhibition was determined by the MTT colorimetric assay. Cells were plated in 96-well plates at a density of 10,000 cells /mL and allowed to attach overnight (16 h). The plates were incubated at 37 °C under a humidified atmosphere containing 5% CO_2 for 72 h. MTT (50 μg) was added and the cells were incubated for another 4 h. Medium/MTT solutions were removed carefully by aspiration, the MTT formazan crystals were dissolved in 100 μL of DMSO, and absorbance was determined on a plate reader at 560 nm. IC_{50} values (concentration at which cell survival equals 50% of control) were determined from semilog plots of percent of control versus concentration.

5.3.2. In vivo antitumor activity

Log-phase MV4-11 cells were harvested, washed 3 times with PBS, followed by resuspension at a concentration of 5 × 10^6 per mL. A total of 100 μL of cell suspension was injected into the flanks of athymic nude mice (7–8 weeks). Tumor sizes were regularly measured using calipers, and volumes were calculated using the following formula: volume (mm^3) = length × width × width/2. After the tumors had grown to 100–150 mm^3, all the mice were randomized into four groups (five mice for each group) in two independent experiments and dosed with **4h** (20 mg/kg and 40 mg/kg), Sunitinib (40 mg/kg), or control. All agents were administered daily for three weeks through tail vein injection, and tumor growth was monitored and measured every day. After three weeks, mice were euthanized and the average tumor volumes were calculated.

Acknowledgments

This work was supported by National Natural Science Foundation of

China (31571901) and grants from the National Key Research and Development Program of China (2017YFD0401301). The authors have no other relevant affiliations or financial involvement with any organization or entity with a financial interest in or financial conflict with the subject matter or materials discussed in the manuscript apart from those disclosed. No writing assistance was utilized in the production of this manuscript.

References

[1] A. Emadi, J.E. Karp, The state of the union on treatment of acute myeloid leukemia, Leukemia Lymphoma 55 (2014) 2423–2425.
[2] B. Oran, D.J. Weisdorf, Survival for older patients with acute myeloid leukemia: a population-based study, Haematologica 97 (2012) 1916–1924.
[3] D.A. Arber, A. Orazi, R. Hasserjian, J. Thiele, M.J. Borowitz, M.M. Le Beau, C.D. Bloomfield, M. Cazzola, J.W. Vardiman, The 2016 revision to the World Health Organization classification of myeloid neoplasms and acute leukemia, Blood 127 (2016) 2391–2405.
[4] H. Dohner, E.H. Estey, S. Amadori, F.R. Appelbaum, T. Büchner, A.K. Burnett, H. Dombret, P. Fenaux, D. Grimwade, R.A. Larson, F. Lo-Coco, T. Naoe, D. Niederwieser, G.J. Ossenkoppele, M.A. Sanz, J. Sierra, M.S. Tallman, B. Lowenberg, C.D. Bloom, Diagnosis and management of acute myeloid leukemia in adults: recommendations from an international expert panel, on behalf of the European LeukemiaNet, Blood 115 (2010) 53–474.
[5] J.P. Patel, M. Gonen, M.E. Figueroa, et al., Prognostic relevance of integrated genetic profiling in acute myeloid leukemia, N. Engl. J. Med. 366 (2012) 1079–1089.
[6] E. Papaemmanuil, M. Gerstung, L. Bullinger, V.I. Gaidzik, P. Paschka, N.D. Roberts, N.E. Potter, M. Heuser, F. Thol, N. Bolli, G. Gundem, P. Van Loo, I. Martincorena, P. Ganly, L. Mudie, S. McLaren, S. O'Meara, K. Raine, D.R. Jones, J.W. Teague, A.P. Butler, M.F. Greaves, A. Ganser, K. Döhner, R.F. Schlenk, H. Döhner, P.J. Campbell, Genomic classification and prognosis in acute myeloid leukemia, N. Engl. J. Med. 374 (2016) 2209–2221.
[7] P.S. Hole, R.L. Darley, A. Tonks, Do reactive oxygen species play a role in myeloid leukemias? Blood 117 (2011) 5816–5826.
[8] B. Carter-Cooper, S. Fletcher, D. Ferraris, E. Choi, D. Kronfli, S. Dash, P. Truong, E. Sausville, R. Lapidus, A. Emadi, Synthesis, characterization and antineoplastic activity of bis-aziridinyl dimeric naphthoquinone – a novel class of compounds with potent activity against acute myeloid leukemia cells, Bioorg. Med. Chem. Lett. 27 (2017) 6–10.
[9] C. Gorrini, I.S. Harris, T.W. Mak, Modulation of oxidative stress as an anticancer strategy, Nat. Rev. Drug Discov. 12 (2013) 931–947.
[10] M.J. Solivio, D.B. Nemera, L. Sallans, E.J. Merino, Biologically relevant oxidants cause bound proteins to readily oxidatively cross-link at Guanine, Chem. Res. Toxicol. 25 (2012) 326.
[11] S. Ohayon, M. Refua, A. Hendler, A. Aharoni, A. Brik, Harnessing the oxidation susceptibility of deubiquitinases for inhibition with small molecules, Angew. Chem. Int. Ed. 54 (2015) 599–603.
[12] X. Zhang, J. Bian, X. Li, X. Wu, Y. Dong, Q. You, 2-Substituted 3,7,8-trimethylnaphtho[1,2-b]furan-4,5-diones as specific L-shaped NQO1-mediated redox modulators for the treatment of non-small cell lung cancer, Eur. J. Med. Chem. 138 (2017) 616–629.
[13] J. Bian, B. Deng, L. Xu, X. Xu, N. Wang, T. Hu, Z. Yao, J. Du, L. Yang, Y. Lei, X. Li, H. Sun, X. Zhang, Q. You, 2-Substituted 3-methylnaphtho[1,2-b]furan-4,5-diones as novel L-shaped ortho-quinone substrates for NAD(P)H:quinone oxidoreductase (NQO1), Eur. J. Med. Chem. 82 (2014) 56–67.
[14] J. Bian, L. Xu, B. Deng, X. Qian, J. Fan, X. Yang, F. Liu, X. Xu, X. Guo, X. Li, H. Sun, Q. You, X. Zhang, Synthesis and evaluation of (±)-dunnione and its orthoquinone analogues as substrates for NAD(P)H:quinone oxidoreductase 1 (NQO1), Bioorg. Med. Chem. Lett. 25 (2015) 1244–1248.
[15] J.L. Bian, X. Li, N. Wang, X.S. Wu, Q.D. You, X.J. Zhang, Discovery of quinone-directed antitumor agents selectively bioactivated by NQO1 over CPR with improved safety profile, Eur. J. Med. Chem. 129 (2017) 27–40.
[16] M. Manickam, P.R. Boggu, J. Cho, Y.J. Nam, S.J. Lee, S. Jung, Investigation of chemical reactivity of 2-alkoxy-1,4-naphthoquinones and their anticancer activity, Bioorg. Med. Chem. Lett. 28 (2018) 2023–2028.
[17] M.F. Cardoso, P.C. Rodrigues, M.E. Oliveira, I.L. Gama, I.M. da Silva, I.O. Santos, D.R. Rocha, R.T. Pinho, V.F. Ferreira, M.C. de Souza, Fde C da Silva, F.P. Silva Jr., Synthesis and evaluation of the cytotoxic activity of 1,2-furanonaphthoquinones tethered to 1,2,3–1H-triazoles in myeloid and lymphoid leukemia cell lines, Eur. J. Med. Chem. 84 (2014) 708–717.
[18] W. Liu, J. Zhou, G. Geng, Q. Shi, F. Sauriol, J.H. Wu, Antiandrogenic, maspin induction, and antiprostate cancer activities of tanshinone IIA and its novel derivatives with modification in ring A, J. Med. Chem. 55 (2012) 971–975.
[19] Y.D. Shen, Y.X. Tian, X.Z. Bu, L.Q. Gu, Natural tanshinone-like heterocyclic-fused ortho-quinones from regioselective Diels-Alder reaction: synthesis and cytotoxicity evaluation, Eur. J. Med. Chem. 44 (2009) 3915–3921.
[20] C. Antczak, D. Shum, B. Bassit, M.G. Frattini, Y. Li, E. de Stanchina, D.A. Scheinberg, H. Djaballah, Identification of benzofuran-4,5-diones as novel and selective non-hydroxamic acid, non-peptidomimetic based inhibitors of human peptide deformylase, Bioorg. Med. Chem. Lett. 21 (2011) 4528–4532.
[21] D. Cedeno, J.J. Bozell, Catalytic oxidation of para-substituted phenols with cobalt–Schiff base complexes/O_2—selective conversion of syringyl and guaiacyl lignin models to benzoquinones, Trtrahedron Lett. 53 (2012) 2380–2383.
[22] C. Morin, T. Besset, J.C. Moutet, M. Fayolle, M. Brückner, D. Limosin, K. Becker, E. Davioud-Charvet, The aza-analogues of 1,4-naphthoquinones are potent substrates and inhibitors of plasmodial thioredoxin and glutathione reductases and of human erythrocyte glutathione reductase, Org. Biomol. Chem. 6 (2008) 2731–2742.
[23] B. Biannic, J.J. Bozell, Efficient cobalt-catalyzed oxidative conversion of lignin models to benzoquinones, Org. Lett. 15 (2013) 2730–2733.
[24] P.G. Cozzi, Metal-Salen Schiff base complexes in catalysis: practical aspects, Chem. Soc. Rev. 33 (2004) 410–421.